Morphological, Crystalline and Photo-luminescent Property of Zinc Oxide Nanorod Array Controlled by Zinc Oxide Sol-gel Thin Film

Jing-Shun Huang* and Ching-Fuh Lin**

*Institute of Photonics and Optoelectronics, National Taiwan University, Taiwan, Republic of China
No. 1, Sec. 4, Roosevelt Road, Taipei, 10617 Taiwan (R.O.C), f92921047@ntu.edu.tw
** Institute of Photonics and Optoelectronics, Graduate Institute of Electronic Engineering and Department of Electrical Engineering, National Taiwan University, Taiwan, Republic of China, cflin@cc.ee.ntu.edu.tw

ABSTRACT

Controllable growth of ZnO nanorod array has been systematically studied. Our investigation demonstrates that the annealing treatment of the ZnO sol-gel thin-film have strong influences on the morphology, crystalline and photoluminescence (PL) of the ZnO nanorod arrays grown thereon. As the annealing temperature increases, the size of the ZnO grain increases, and the diameter of thereon ZnO nanorod arrays increases from 60 to 250 nm. Besides, the growth rate of ZnO nanorod is very sensitive to the ZnO grains, and then influences the PL peak at 380 nm. The x-ray diffraction spectra indicate that the thin film annealed at the low temperature of 130 ℃ is amorphous, but the thereon nanorod arrays are high-quality single crystals growing along the c-axis direction with an orientation perpendicular to the substrates. The as-synthesized ZnO nanorod arrays via all solution-based processing enable the fabrication of next-generation nano-devices at low temperature.

Keywords: nanorods, zinc oxide, morphology, sol-gel, hydrothermal, photoluminescence, crystallinity

1 INTRODUCTION

Zinc oxide (ZnO) is a II-VI compound oxide semiconductor with a direct band gap of 3.37 eV and a large exciton binding energy of 60meV at room temperature, exhibiting near-UV light emission, transparent conductivity, and piezoelectricity. It has attracted great interest for promising applications in optoelectronics devices such as room temperature lasers [1], light emitting diodes [2], ultraviolet (UV) detectors [3], field emission displays [4], photonic crystals [5], and solar cells [6, 7], especially in the form of one-dimensional nanowires, nanorods, or nanotubes. In view of this point, controlled growth of ZnO nanostructures in terms of morphology and orientation is of significant importance from the standpoint of both basic fundamental research and the development of novel devices. To date, various synthesis approaches have been demonstrated to fabricate ZnO nanorods, which can be classified into two categories, vapor-phase and solution-phase methods. Vapor-phase processes such as vapor-liquid-solid epitaxy (VLSE), chemical vapor deposition (CVD), and pulse laser deposition (PLD) have some limitations for substrate size and the need for high temperature operation [8, 9]. For these reasons, there is a significant need to develop a low-temperature, large-scale, versatile route to synthesis of ZnO nanorods. Solution-phase methods are appealing due to their low growth temperature, low cost, and potential for scale-up. Recently, growth of ZnO nanorods in aqueous solutions at low temperature was reported by using the hydrothermal process [10]. Hydrothermal process has shown the possibility for applications in light emitting diodes and solar cells with their growth temperature below 100 ℃ and easy scale-up. This aqueous-based technique has also been used successfully to demonstrate the fabrication of large arrays of vertical ZnO nanorods on glass and plastic substrates [11]. This stimulated the study of using ZnO nanorod arrays on plastic substrates for application in flexible electronic devices.

C. Bekeny *et al.* [12] reported that the size of ZnO nanorods varied with the composition of the chemical precursors. M. Guo *et al.* [13] reported that the diameter and length of ZnO nanorod arrays were controlled at different growth temperatures under hydrothermal conditions. X. Wang *et al.* [14] reported that an annealing treatment of the substrate can influence the density of the ZnO nanorod arrays on indium tin oxide (ITO), but there is no study on crystallinity and photoluminescence (PL) of ZnO nanorod arrays. However, systematic research on the effect of quality characteristics of ZnO sol-gel thin films on the growth of ZnO nanorod arrays has rarely been reported.

In this work, we systematically study the feature-controlled ZnO nanorod arrays via hydrothermal method using ZnO sol-gel thin films were used as the seed layers with different pretreatment conditions. Our investigation shows that the vertical alignment, the crystallinity, and the growth rate of ZnO nanorod arrays are strongly dependent on the characteristics of the thin films. Field-emission scanning electron microscopy (FESEM), x-ray diffraction (XRD) pattern, and room temperature PL spectrum were applied to analyze the quality of the ZnO nanorod arrays.

2 EXPERIMENTAL DETAIL

2.1 Preparation of ZnO sol-gel thin films

The ZnO thin films was deposited on silicon substrates by a sol-gel method as previously reported in the literature [15]. A coating solution contained zinc acetate dihydrate [Merck, 99.5% purity] and equivalent molar monoethanolamine (MEA) [Merck, 99.5% purity] dissolved in 2-methoxyethanol (2MOE) [Merck, 99.5% purity]. The concentration of zinc acetate was 0.5 M. The resulting solution was then stirred at 60 ℃ for 2 hours to yield a homogeneous and stable solution, which served as the coating solution after being cooled to room temperature. Then the solution was spin-coated onto p-type silicon (100) substrates at the rate of 1000 rpm for 20 s and then 3000 rpm for 30 s at room temperature. Subsequently, the gel films were preheated for 10 minutes to remove the residual solvent. Then the films were annealed in a furnace at different temperatures ranging from 130 ℃ to 900 ℃ for one hour.

2.2 Growth of ZnO nanorod arrays

After uniformly coating the silicon substrates with ZnO thin films, hydrothermal growth of ZnO nanorod arrays was achieved by suspending these ZnO seed-coated substrates upside-down in a glass beaker filled with aqueous solution of 50 mM zinc nitrate hexahydrate [Sigma Aldrich, 98% purity] and 50 mM hexamethylenetetramine (HMT) [Sigma Aldrich, 99.5% purity]. During the growth, the glass beaker was heated with an oven and maintained at 90 ℃ for 4 hours. At the end of the growth, the substrates were removed from the solution, then rinsed with de-ionized water to remove any residual salt from the surface, and dried under nitrogen gas flow.

2.3 Characterization of ZnO thin films and thereon ZnO nanorod arrays

The general morphologies of the ZnO thin films and thereon ZnO nanorod arrays were examined by FESEM. The crystal phase and crystallinity were analyzed at room temperature by XRD using Cu Kα radiation. The room temperature PL, measured using a Nd:YAG laser at 266nm as the exciting source, was used to characterize the optical properties of the thereon ZnO nanorod arrays.

3 RESULTS AND DISCUSSIONS

3.1 ZnO sol-gel thin films

Figure 1 shows the top view FESEM images for the surface morphologies of ZnO sol-gel thin films with increasing annealing temperatures from 130 to 900℃. At the annealing temperature of 130 ℃, no grain forms and the surface is smooth. At the annealing temperature of 300 ℃, the film contains fine grains and the particle size is about 80nm. Once the annealing temperature increases, the grains become larger and densely packed. It demonstrates that the grain size of the ZnO thin film was changed due to re-distribution of crystalline grain by supplying sufficient thermal energy and the small grain has been joined into great crystalline surface.

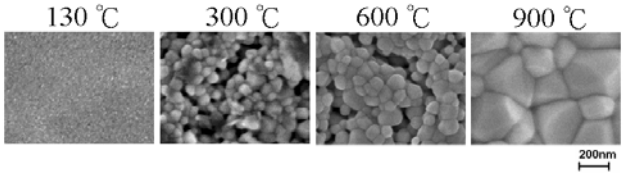

Figure 1: FESEM images of ZnO sol-gel thin films with annealing temperature from 130 to 900 ℃.

Figure 2 gives the XRD patterns of those ZnO thin films annealed at 130, 300, 600 and 900 ℃, respectively. The XRD patterns reveal that the (002) peak intensity varies with annealing temperature. When the ZnO thin films are annealed below 300 ℃, there is no preferred (002) *c*-axis orientation. At the temperature of 600 ℃, (100), (002), and (101) diffraction peaks corresponding to the ZnO wurtzite structure are observed in the XRD pattern, where the preferred (002) *c*-axis orientation dominates. When the annealing temperature increases to 900 ℃, the polycrystalline structure emerges with the (100) and (101) peaks while the intensity of the (002) peak decreases. This result indicates that the crystalline quality of each grain becomes poor [16]. Therefore, it maybe concluded that the preferred *c*-axis orientation initially increases with annealing temperature until it reaches the optimal situation at a certain annealing temperature. Afterwards the *c*-axis orientation intensity decreases gradually.

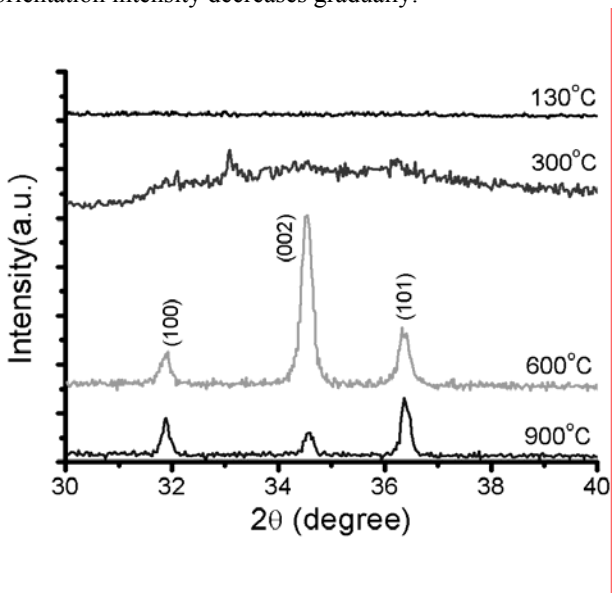

Figure 2: X-ray diffraction spectra of ZnO thin films annealed from 130 to 900 ℃

3.2 ZnO nanorod arrays

The as-grown ZnO nanorod arrays are shown in Figure 3. The obtained ZnO nanorod arrays are typically hexagonal-shaped. As the annealing temperatures of the ZnO thin films increase from 130 to 900 ℃, the diameters of the ZnO nanorod arrays increase from 60 to 260 nm (Figure 4). The reason may be that the high annealing temperature enhances the interaction among the grains and leads the grains to merge together to form bigger ZnO seeds, and thus increases the diameter of the ZnO nanorods thereon. Therefore, the size of the grains is a key factor that affects the nucleation of ZnO nanorod arrays. Furthermore, the ZnO nanorod arrays on the ZnO thin films annealed at 130 ℃ are well-aligned vertically and uniformly, and the well-defined crystallographic planes of the hexagonal single-crystalline nanorods can be clearly identified, providing evidence that the nanorod arrays orientate along the *c*-axis.

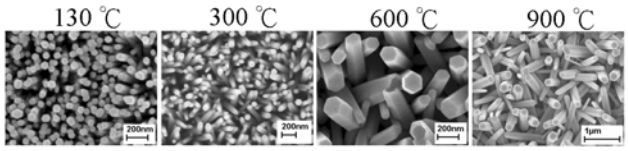

Figure 3: FESEM images of ZnO nanorod arrays grown at 90 ℃ with the thin films annealed from 130 to 900 ℃.

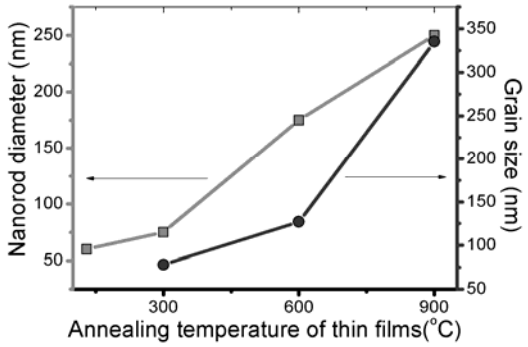

Figure 4: Dependence of the ZnO nanorod diameter (rectangles) and grain size of ZnO thin film (circles) on annealing temperature of ZnO thin films.

Figure 5 shows the XRD patterns of the ZnO nanorod arrays corresponding to those shown in Figures 2. Please note again that the nanorod arrays are grown at the same temperature of 90℃, while the thin films were annealed from 130 to 900 ℃. The peaks in the x-ray diffraction patterns are indexed to the hexagonal phase of ZnO. It is found that no other characteristic peaks corresponding to the impurities of the precursors such as zinc nitrate and zinc hydroxide are observed in the XRD patterns. At the temperature of 130, 300, and 600 ℃, only a very strong (002) diffraction peak and a very weak (101) peak are observed, indicating that the three ZnO samples are all of high *c*-axis orientation. It is noticeable that for the sample annealed at 130 ℃, the XRD pattern shows only the (002) diffraction peak. In addition, the intensity of (002) diffraction peak is strongest, compared to other samples annealed at higher temperatures. This implies its perfect *c*-axis orientation and this result is in accordance with its SEM image. On the other hand, for the sample annealed at 900 ℃, the (002) diffraction peak becomes weak, and at the same time, the (100) and (101) peaks become strong, indicating its tendency toward random orientation. It means that the films annealed at 900 ℃ has worse morphology and hence results in the relatively random orientation of nanorod arrays as observed in the Figure 3.

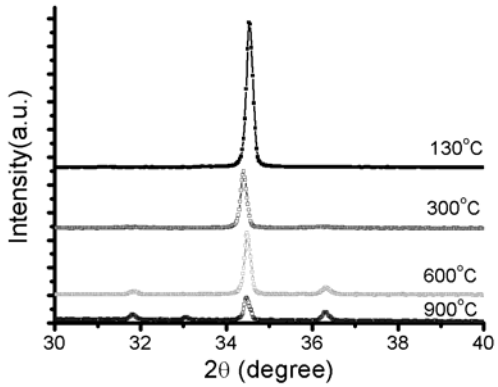

Figure 5: X-ray diffraction spectra ZnO nanorod arrays with ZnO thin films annealed from 130 to 900 ℃.

It is interesting to note that the (002) diffraction peak of the seed layer annealed at 130 ℃ is smaller than the others, while the (002) diffraction peak of thereon ZnO nanorod arrays at 130 ℃ is larger than the others. The previous investigation of the thin films annealed at 130℃ indicates that it is nearly amorphous. However, the growth of ZnO nanorod arrays on amorphous ZnO thin films along the (002) plane is even more notable than that on poly-crystalline thin films. It may be because the poly-crystalline ZnO grains with a certain orientation limit the growth along the (002) plane. In comparison, the amorphous ZnO seed layer does not limit the growth along the (002) plane. This indicates that the ZnO nanorod arrays prepared by the hydrothermal method have preferential orientation along the (002) plane, in particular on the thin films without a certain orientation.

3.3 Annealing effect of ZnO thin films on PL spectra of thereon ZnO nanorod arrays

The room temperature PL characteristics of as-grown ZnO nanorod arrays with different annealing temperatures of thin films are shown in Figure 6. The UV peak increases with annealing temperature. The UV emission of ZnO nanorod arrays corresponding to the near band edge emission is due to the recombination of free excitons

through an exciton-exciton collision process. At the temperature of 900 ℃, the defect-related green emission of the nanorod arrays is lower than that of the seed layers. The green emission is also known to be a deep level emission caused by the impurities and structural defects in the crystal such as oxygen vacancies, zinc interstitials, and so on [17].

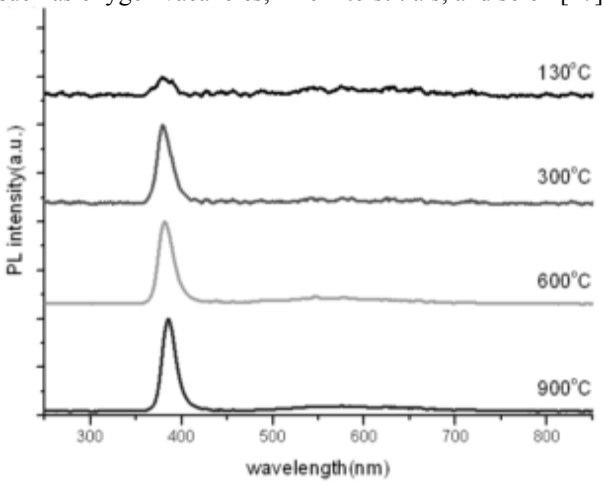

Figure 6: Room temperature PL spectra of ZnO nanorod arrays with ZnO thin films annealed from 130 to 900 ℃.

Moreover, as shown in Figure 7, the sample annealed at high temperature of 900 ℃ has both larger size of ZnO nanorod arrays and stronger PL intensity at 380 nm, while the sample annealed at low temperature of 130 ℃ has both smaller nanorod size and weaker PL intensity. As a result, the growth rate of ZnO nanorods along the c-axis direction is very sensitive to the size of ZnO grains, and then influences the PL peak at 380 nm.

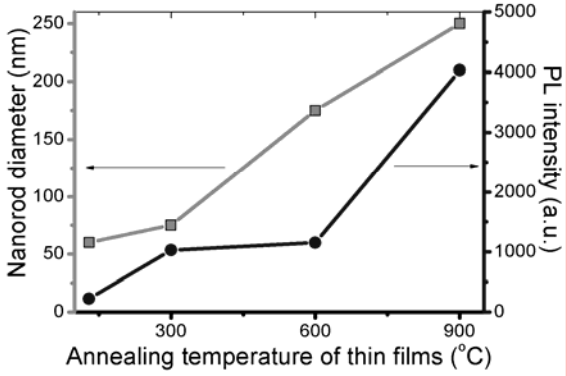

Figure 7: Diameter (rectangles) and PL intensity at 380 nm (circles) of ZnO nanorods as functions of annealing temperature of ZnO thin films.

4 CONCLUSIONS

This work provides a systematic study of controlled growth of ZnO nanorod arrays by using the hydrothermal method. Our investigation demonstrates that the annealing treatment of ZnO sol-gel thin films have strong influences on the diameter and orientation of the ZnO nanorod arrays grown thereon. The annealing temperature of the ZnO thin films can affect the microstructure of the ZnO grains and then the growth of the ZnO nanorod arrays. As the annealing temperature increases from 130 to 900 ℃, the grain size of the thin films increases, and the diameter of thereon ZnO nanorod arrays increases. The thin films influence the nucleation of the ZnO and subsequently affect the diameter and orientation of the thereon nanorod arrays. At the temperature of 130 ℃, the ZnO nanorod arrays align very vertically with growth along the *c*-axis direction. This work provides a route to fabrication of low-cost highly oriented ZnO nanorod arrays at low temperature. These vertical nanorod arrays are highly suitable for use in ordered nanorod-polymer devices, such as solar cells and light emitting diodes.

ACKNOLEDGEMENT

This work was supported by the National Science Council, Taiwan, Republic of China, with Grant NOs. NSC96-2221-E-002-277-MY3 and NSC96-2218-E-002-025.

REFERENCES

[1] M. H. Huang *et al.*, Science 292, 1897 (2001).
[2] S. H. Park, S. H. Kim, and S. W. Han, Nanotechnology 18, 055608 (2007).
[3] C. Y. Lu *et al.*, Applied Physics Letters 89, 153101 (2006).
[4] B. Cao *et al.*, Journal of Physical Chemistry C 111, 2470 (2007).
[5] J. Cui, and U. Gibson, Nanotechnology 18, 155302 (2007).
[6] K. Takanezawa *et al.*, Journal of Physical Chemistry C 111, 7218 (2007).
[7] J. J. Wu *et al.*, Applied Physics Letters 90, 213109 (2007).
[8] M. H. Huang *et al.*, Advanced Materials 13, 113 (2001).
[9] G. Z. Wang *et al.*, Materials Letters 59, 3870 (2005).
[10] L. Vayssieres, Advanced Materials 15, 464 (2003).
[11] J. B. Cui *et al.*, Journal of Applied Physics 97, 044315 (2005).
[12] C. Bekeny *et al.*, Journal of Applied Physics 100, 104317 (2006).
[13] M. Guo *et al.*, Journal of Solid State Chemistry 178, 3210 (2005).
[14] T. Ma *et al.*, Nanotechnology 18, 035605 (2007).
[15] M. Ohyama, H. Kouzuka, and T. Yoko, Thin Solid Films 306, 78 (1997).
[16] X. Q. Wei *et al.*, Materials Chemistry and Physics 101, 285 (2007).
[17] Q. Ahsanulhaq, A. Umar, and Y. B. Hahn, Nanotechnology 18, 115603 (2007).